Mechanisms of N-acetylcysteine in reducing monocrotaline-induced pulmonary hypertension in rats: Inhibiting the expression of Nox1 in pulmonary vascular smooth muscle cells

WENCHENG YU[1], WEINA JI[1], LIYUN MI[1] and CHEN LIN[2]

[1]Department of Respiratory Diseases, The Affiliated Hospital of Qingdao University, Qingdao, Shandong 266003; [2]Department of Respiratory Diseases, Shenli Oilfield Central Hospital, Dongying, Liaoning 257064, P.R. China

Received June 7, 2016; Accepted May 30, 2017

DOI: 10.3892/mmr.2017.7326

Abstract. The aim of the present study was to investigate the impact of N-acetylcysteine (NAC) on the expression of reduced nicotinamide adenine dinucleotide phosphate oxidase 1 (Nox1), and the proliferation and apoptosis of pulmonary artery smooth muscle cells (PASMCs) in rats exhibiting monocrotaline (MCT)-induced pulmonary hypertension, and to investigate the possible mechanisms and treatment roles of NAC in pulmonary vascular remodeling (PVR). A total of 18 Wistar rats were randomly divided into three groups: The control (C) group; the MCT (M) group; and the NAC (N) group. The right ventricular hypertrophy index (RVHI) and other indicators were recorded 6 weeks subsequently. Groups C and M were divided into two subgroups: Groups C1 and M1 (control); and group C2 and M2 group (treated with ML171). Group N was not sub-divided. PASMCs were isolated, and the vascular remodeling and Nox1 positioning were observed. The expression of Nox mRNA in each group, and the proliferation, apoptosis, and superoxide dismutase (SOD) activity of PASMCs, prior to and following the ML171 treatment, were measured. NAC was able to decrease RVHI and other indicators ($P<0.001$). The mRNA expression of Nox1 and Nox4 in group M was significantly increased compared with group C ($P<0.05$), and NAC was able to significantly decrease the expression of these two factors in lung tissue ($P<0.001$). MCT-PASMCs exhibited differences in Nox1 mRNA expression ($P<0.001$), and the total SOD activity was Nox1-dependently increased ($r=0.949$; $P<0.001$). NAC was able to decrease Nox1-derived reactive oxygen species in PASMCs, thereby improving PVR. Nox1 was able to increase SOD activity, thereby demonstrating its positive effect on the proliferation of MCT-PASMCs.

Correspondence to: Dr Wencheng Yu, Department of Respiratory Diseases, The Affiliated Hospital of Qingdao University, 16 Jiangsu Road, Qingdao, Shandong 266003, P.R. China
E-mail: wenchengyudoc@163.com

Key words: N-acetylcysteine, pulmonary hypertension, oxidative stress, reduced nicotinamide adenine dinucleotide phosphate oxidase 1, vascular remodeling

Introduction

Pulmonary hypertension (PH) is defined as a mean pulmonary artery pressure (mPAP) ≥25 mmHg, measured via right heart catheter at rest. PH may be fatal, and the natural course of idiopathic pulmonary artery hypertension (PAH) is 2.5-3.4 years following diagnosis (1). The pathogenesis of PAH is not completely clear, and appears to be primarily associated with heredity and immune-based pulmonary vascular remodeling (PVR) (2,3). Accepted therapeutic approaches for PAH primarily target vasoconstriction, intimal injury or cardiac dysfunction. However, PVR must be reversed in order to cure PAH.

Stimuli which may lead to vascular remodeling include transmural pressure, mechanical stretching or hypoxia, and repeated insults from these damaging factors cause a state of oxidative stress; the production of reactive oxygen species (ROS) is increased and ROS clearance is decreased, thereby inducing oxidative injury (4). reduced nicotinamide adenine dinucleotide phosphate oxidase (Nox) is one of the primary sources of ROS, and alterations in its expression have been demonstrated to be associated with pulmonary vascular disease and the survival of patients with PAH (2). The experimental model of hypoxia-induced pulmonary hypertension has been widely-used, but few studies have used the monocrotaline-induced pulmonary hypertension (MCT-PH) model to study Nox-derived ROS (4). The PAH-associated Nox family of proteins includes Nox1 and Nox4, although conflicting reports exist on the roles of Nox1 and Nox4 in the occurrence and development of PAH (5,6). Previous studies have used different cell and tissue samples; therefore, the present study analyzed the Nox1 and Nox4 expression levels in lung tissue homogenate and pulmonary artery smooth muscle cells (PASMCs), aiming to investigate whether the differences observed in regulatory mechanisms were caused by different samples, modeling methods or pathogenic mechanisms.

Previous studies into PAH have focused on the antioxidant enzyme superoxide dismutase (SOD), the role of which is to

catalyze the conversion of O_2^- to O_2 and H_2O. During this process, two molecules of glutathione (GSH) are oxidized (7). N-acetylcysteine (NAC) is a synthetic precursor of GSH, which exhibits antioxidant properties and has been clinically applied for the treatment of idiopathic pulmonary fibrosis and ischemia reperfusion injury (8-10). A previous study demonstrated that NAC was able to improve PH and right ventricular function via immune regulatory mechanisms (11). Therefore, it was hypothesized that NAC may protect against oxidation, thereby alleviating MCT-induced pulmonary vascular and right heart diseases. The possible mechanisms underlying the role of NAC in treating PAH were investigated in the present study.

Materials and methods

Grouping and establishment of PH rat model. A total of 18 8-week-old male Wistar rats (Central Laboratory, Affiliated Hospital of Qingdao University, Qingdao, China), weighing 150-180 g, were randomly divided into three groups (n=6): Rats in the control group received one intraperitoneal injected with 60 mg kg^{-1} saline; those in the MCT group were intraperitoneally injected once with 60 mg kg^{-1} MCT (Sigma-Aldrich; Merck KGaA, Darmstadt, Germany); and those in the NAC group intraperitoneally injected once with 60 mg kg^{-1} MCT, and orally administered 500 mg kg^{-1} d^{-1} NAC (Sigma-Aldrich; Merck KGaA). The control and MCT groups were orally administered 500 mg kg^{-1} d^{-1} saline. All of the rats were fed under the same conditions (temperature 22±2˚C, 12-h light/dark cycle and food and water *ad libitum*) and medicated for 6 weeks. The right ventricular systolic pressure (RVSP) and mPAP of each rat was subsequently measured using a right heart catheterized polygraph (AD Instruments Pty., Ltd., Bella Vista, Australia). The present study was performed in accordance with the recommendations in the Guide for the Care and Use of Laboratory Animals of the National Institutes of Health (Bethesda, MA, USA). The animal use protocol was reviewed and approved by the Institutional Animal Care and Use Committee of Qingdao University.

Tissue and cell preparation. The rats were sacrificed, and the pulmonary arteries were isolated. Following rinsing with saline at 37˚C, the upper left lung lobe was fixed for 12 h in 10% neutral formalin, followed by paraffin-embedding and slicing; PASMCs were isolated from the lower left lung lobe using D-Hank's solution (Hefei Bomei Biotechnology Co., Ltd., Hefei, China). The right lung was rapidly frozen in liquid nitrogen prior to extraction of RNA and proteins. The heart was removed, and the right ventricle (RV) and left ventricle plus septum (LV + S) were separated for weighing.

Following rinsing in PBS, the distal pulmonary artery was separated from the lower left lung lobe and the PASMCs were purified to produce a cell suspension. The first generation was identified using immunofluorescence staining of smooth muscle actin with polyclonal anti-α-SMA antibody (A03744; 1:1,000; Wuhan Boster Biological Technology, Wuhan, China) incubated overnight at 4˚C, and the second generation was used for subsequent experiments. The obtained PASMCs was divided into three groups: Group C, isolated from the saline-treatment group; Group M, isolated from the MCT-treatment group; and group N, isolated from the NAC-treatment group. Groups C and M were sub-divided: Subgroups C1 and M1 (control), pretreated with an equal volume of PBS solution for 24 h; subgroups C2 and M2, pretreated with 100 μmol l^{-1} ML171 (Merck KGaA) for 24 h. Group N was not subdivided (blank control).

Dihydroethidium (DHE) fluorescence staining. The cryopreserved lung tissue was embedded in optimal cutting temperature compound (Beijing Kangwei Century Biological Technology Ltd., Beijing, China), followed by sectioning at 20 μm at -20˚C and DHE fluorescence staining (Nanjing KeyGen Biotech Co., Ltd., Nanjing, China) at 37˚C for 1 h. A fluorescence microscope (BX51; Olympus Corporation, Tokyo, Japan) was used for the observation (magnification, x400), and the images were analyzed using Image Pro Plus software version 6.0 (Media Cybernetics, Inc., Rockville, MD, USA).

Observation of pulmonary vascular structures. Each paraffin block of rat lung tissue was cut into 3-μm-thick sections, followed by xylene dewaxing and graded alcohol rehydration for hematoxylin and eosin (HE) staining (25˚C for 10 min). Each section was observed in three visual fields with a fluorescence microscope, and 10 antero-capillary pulmonary arteries with a diameter <50 μm (determined according to the results of the α-SMA immunofluorescence staining). were selected for analysis of pulmonary vascular structure, medial thickness and degree of muscularization, using Image Pro Plus software version 6.0 (Media Cybernetics, Inc.).

Expression and localization of Nox1. The 3-μm slice preparation was the same as for the HE staining. The slices were rinsed with PBS, goat blocking serum (AR1009; Boster Biological Technology) was applied and the slices were incubated at room temperature for 30 min. Excess serum was absorbed and primary anti-Nox1 antibody (BA3720; 1:100; Boster Biological Technology) added for overnight incubation at 4˚C. Subsequently, the sections were rinsed three times in PBS and the secondary antibody, Cy3 conjugated anti-mouse IgG (BA1031; 1:100; Boster Biological Technology), was applied and incubated for 2 h at 37˚C. The primary anti-α-SMA antibody and secondary antibody, HRP conjugated anti-mouse IgG (LK2003; 1:100; Tianjin Sungene Biotech Co., Ltd., Tianjin, China), were added following the same protocol and the excess dye was rinsed out using PBS, followed by mounting the section in neutral gum. A fluorescence microscope was used for observation, and the results were analyzed using Image Pro Plus software.

Reverse transcription-quantitative polymerase chain reaction (RT-qPCR). The RNA of Nox1 and Nox4 were extracted (TRIzol, Beijing Kaiao Technology Development Co., Ltd., Beijing, China) from the lung tissue homogenates of the control, MCT and NAC groups, and from the PASMCs of the N and C groups; RNA was additionally extracted from the PASMCs of the C2 and M2 groups. The RNA concentration and degree of degradation was determined using colorimetry and electrophoresis, respectively. RT was performed using an RT kit (EzOmics SYBR qPCR kit;

Promega Corporation, Madison, WI, USA) and the resulting cDNA was purified using the PCR Purification kit (Qiagen GmbH, Hilden, Germany). The primers were designed and synthesized by Beijing Kaiao Technology Development Co., Ltd. The cDNA was amplified for 40 cycles, and the cycles in each well were 20 sec at 90˚C; 20 sec at 55˚C and 20 sec at 72˚C). The mRNA expressions of different samples were quantified using the $2^{-\Delta\Delta Cq}$ method (12). The primer sequences were as follows: Hypoxanthine phosphoribosyltransferase forward, 5'-CTCAGTCCCAGCGTCGTGAT-3', reverse, 5'-AGCACACAGAGGGCCACAAT-3'; Nox1 forward, 5'-ATGGTCCCTTTGGCACAGTC-3', reverse, 5'-ATCCCAGCCAGTGAGGAAGA-3'; and Nox4 forward, 5'-CCAGTGGTTTGCAGACTTGC-3', reverse, 5'-CGAGGACGCCCAATAAAAAG-3'.

Western blot analysis. Total protein was obtained using Pierce protein extraction buffer (Thermo Fisher Scientific, Inc., Waltham, MA, USA) from the lung tissue homogenates of the control, MCT and NAC groups, and from the PASMCs of groups C1, M1, and N, via centrifugation (21,952 x g for 10 min at 23˚C). Total protein was quantified using the Bradford method and 15 μg protein/lane was separated via SDS-PAGE on an 8% gel. The separated proteins were transferred onto a nitrocellulose membrane and Ponceau staining (0.2% for 10 min at 4˚C) was performed, followed by ≥1 h blocking in skimmed milk at 4˚C. Membranes were incubated with anti-Nox1 polyclonal antibody for 12 h at 4˚C and washed in TBS with Tween-20 (TBST). The labeled secondary antibody, Cy3 conjugated anti-mouse IgG (BA1031; 1:100; Boster Biological Technology), was then added and incubated at room temperature for 2 h, followed by washing with TBST. The specific bands were detected using chemiluminescence (Beijing Kaiao Technology Development Co., Ltd.) and developed onto X-ray films. Each sample was repeated ≥3 times. TotalLab TL 100 program (Nonlinear Dynamics, Newcastle, UK) was used to analyze the specific bands, with β-actin (BM0670; 1:100; Boster Biological Technology) as the internal control.

Detection of cell proliferation and apoptosis. The proliferation assay was performed on groups C1, M1, N1, C2 and M2, according to the manufacturer's protocol of the BrdU Cell Proliferation Assay kit (Roche Diagnostics, Basel, Switzerland). Each sample was repeatedly tested ≥3 times, and the count/minute values were obtained using a liquid scintillation counter (Beckman Coulter, Inc., Brea, CA, USA). The apoptosis assay was performed on groups C1, M1, N1, C2 and M2. The total protein was extracted using the western blotting method and subsequently quantified. The caspase-3 activity was detected using a colorimetric kit (CaspACE colorimetric assay kit; Promega Corporation), according to the manufacturer's protocol. Each sample was assayed in three repeated wells. The protein-free control group was additionally assayed, and the optical density was measured at 405 nm with a microplate reader. The differences between the mean of each group and that of the control group were used to evaluate the caspase-3 activity in each group.

Detection of total SOD activity. The total SOD activity in groups C1, M1, N1, C2 and M2 was detected. The cells were collected, lysed and centrifuged at 4˚C to obtain the supernatant as the test sample. The working solutions were prepared according to the manufacturer's protocol of the SOD activity detection kit (Beyotime Institute of Biotechnology, Haimen, China). 96-well plates were used to set up sample wells and blank control wells. The absorbance at 450 nm was measured (VU2450 visible spectrophotometer; Shimadzu Corporation, Kyoto, Japan) and the inhibition percentage was calculated.

Statistical analysis. The results are expressed as the mean ± standard deviation. For the normally distributed data, the intergroup comparisons were performed using analysis of variance followed by Fisher's least significant difference test. The correlation was analyzed using Pearson's correlation analysis, with the test level set as α=0.05. P<0.05 was considered to indicate a statistically significant difference. All of the results were analyzed using SPSS software (version 19.0; IBM Corp., Armonk, NY, USA).

Table I. Hemodynamics and right heart hypertrophy index.

	Group C	Group M	Group N
RVSP, mmHg	19.78±1.84	51.56±1.44[a]	28.72±1.93[b]
mPAP, mmHg	20.13±1.75	49.10±1.24[a]	26.87±2.58[b]
RV/LV+S	0.22±0.11	0.85±0.08[a]	0.30±0.36[b]
WT, %	53.66±0.54	57.28±0.62[a]	54.20±0.44[b]

Data are presented as the mean ± standard deviation. [a]P<0.001 vs. Cont; [b]P<0.001 vs. MCT. RVSP, right ventricular systolic pressure; mPAP, mean pulmonary artery pressure; RV/LV+S, right ventricle/left ventricle + septum; WT, membrane thickness in the small pulmonary artery; C, control; M, monocrotaline-treated; N, N-acetylcysteine-treated.

Results

Alterations in hemodynamic parameters, pulmonary vascular structures and RVHI. Following a single intraperitoneal injection of MCT, mPAP was increased from 20.13±1.75 to 49.10±1.24 mmHg (P<0.001), in addition to a significant increase in RVSP, from 19.78±1.84 to 51.56±1.44 mmHg (P<0.001), and right ventricular hypertrophy. The measuring index was the increased RV/LV+S ratio, which was increased from 0.22±0.11 to 0.85±0.08 (P<0.001), indicating that the rat PAH model was successfully generated (Table I). Compared with group M, group N exhibited significantly decreased mPAP and RVSP, but the right ventricular functions were improved (Table I), and the degree of medial thickening and PVR were decreased (Fig. 1).

Expression of Nox1 and Nox4 in PASMCs, and positioning of Nox1. As presented in Fig. 2, PASMC was the primary location of vascular remodeling in MCT-PAH. In order to clarify the roles of Nox1 and Nox4 in PAH, the mRNA expression of Nox1 and Nox4 was measured in healthy and MCT-treated rat lung tissue homogenates and PASMCs by RT-qPCR. Nox1 and Nox4 were detected in PASMCs of the MCT and control groups, and in the MCT-treated lung tissue homogenates, Nox1

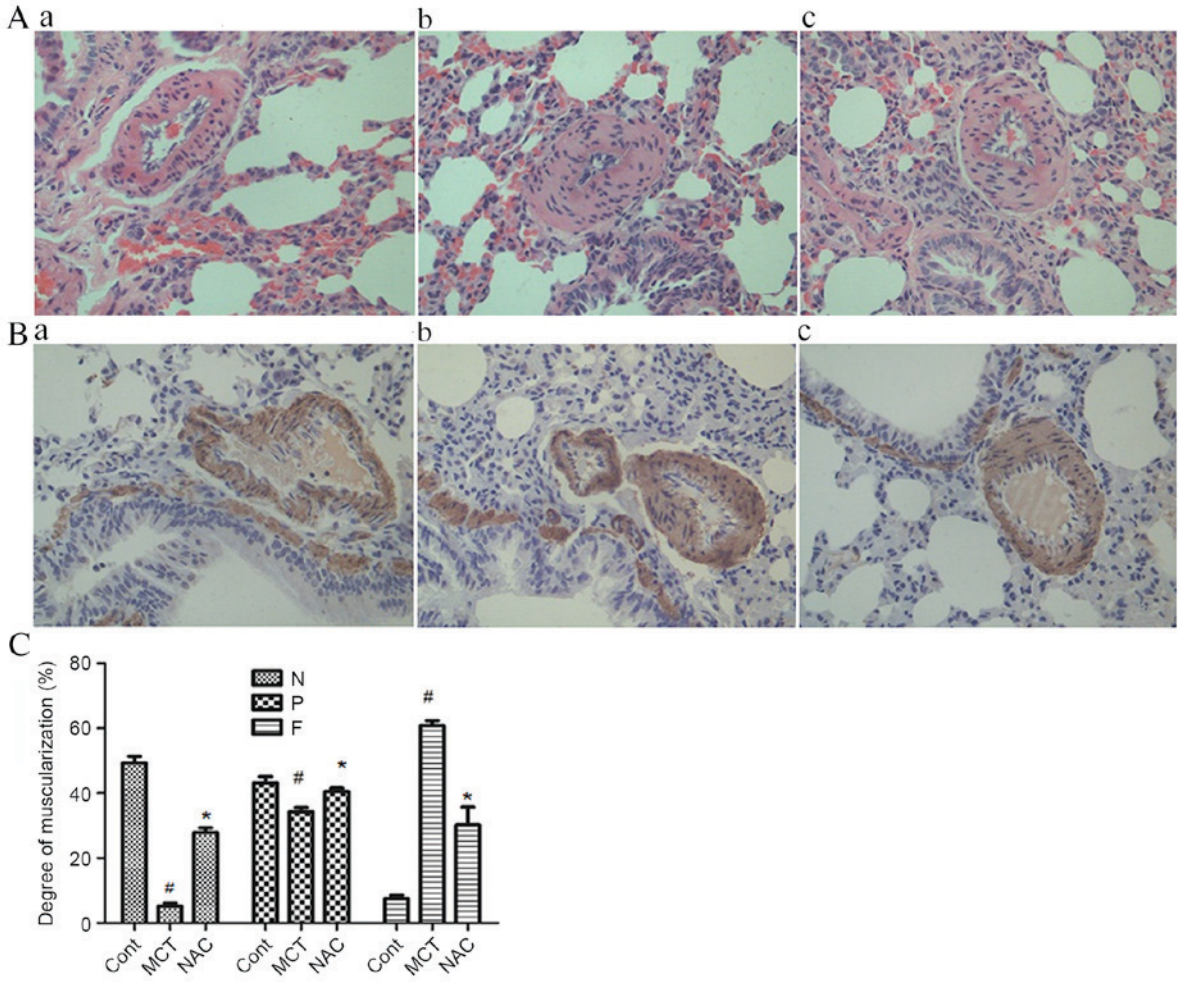

Figure 1. Analysis of muscularization of pulmonary vasculature. (A) Hematoxylin and eosin staining of lung tissue (magnification, x200). (B) Immunofluorescence staining of lung tissue (magnification, x400). Green, smooth muscle actin. (C) The muscle percentage of pulmonary vascular (n=6). #P<0.001 vs. Cont; *P<0.001 vs. MCT. Cont, control; MCT, monocrotaline; NAC, N-acetylcysteine; N, nonmuscularized; P, partially muscularized; F, fully muscularized.

and Nox4 were significantly upregulated (Fig. 2A; P<0.05); however, in PASMCs, the expression of Nox4 in the MCT group and control groups exhibited no significant difference (Fig. 2B). The significant upregulation of Nox1 was additionally confirmed at the protein level (Fig. 2D and E; P<0.05). Following the NAC treatment, compared with the MCT group, the expression of Nox1 and Nox4 in lung tissues was significantly decreased (Fig. 2A; P<0.05), whereas in PASMCs, only Nox1 was decreased significantly (Fig. 2B; P<0.05). The results of α-SMA and Nox1 dual immunofluorescence staining (Fig. 2C) demonstrated that in MCT-PAH, Nox1 was primarily expressed in PASMCs, and the alterations in DHE fluorescence intensity were positively correlated with the protein expression changes of Nox1 (r=0.850; P<0.001; Fig. 2F and H).

Impact of Nox1 on proliferation and apoptosis. The MCT-treated PASMCs exhibited significantly increased cell proliferation, but NAC was able to significantly decrease cell proliferation (Fig. 3A; P<0.001). The apoptotic rates of PASMC among the three groups exhibited no significant difference (Fig. 3B; P>0.05). Following treatment with the Nox1 inhibitor ML171, the proliferation of PASMCs in groups C1 and M1 were significantly decreased compared with C2 and M2 (Fig. 3C and D; P<0.001).

Total SOD activity. In response to oxidative stress, it was hypothesized that the alterations in cellular antioxidant capacities may be observed. The SOD activity was significantly increased in MCT-PASMCs and, compared with group M1, group N1 exhibited decreased SOD activity rather than the expected increase (Fig. 4A; P<0.05). The total SOD activity was decreased by the inhibition of Nox1 (Fig. 4B and C; P<0.05). Therefore, the total SOD activity was dependent on Nox1. The correlation between SOD activity and cell proliferation demonstrated that SOD was significantly correlated with the proliferation of PASMCs (Fig. 4D; r=0.949; P<0.001).

Discussion

Due to the unknown etiology, there remains a lack of effective treatments for PAH and the prognosis is poor. The primary mechanisms are the increasing of pulmonary vascular resistance and pulmonary arterial pressure caused by the changes of pulmonary vascular structures, thickening of the tunica media, stenosis and non-muscle vascular muscularization, which eventually lead to right heart failure. During this process, the proliferative and apoptotic alterations of PASMCs are determined, and ROS serve important roles in this process (3). However, whether ROS are upregulated or downregulated in

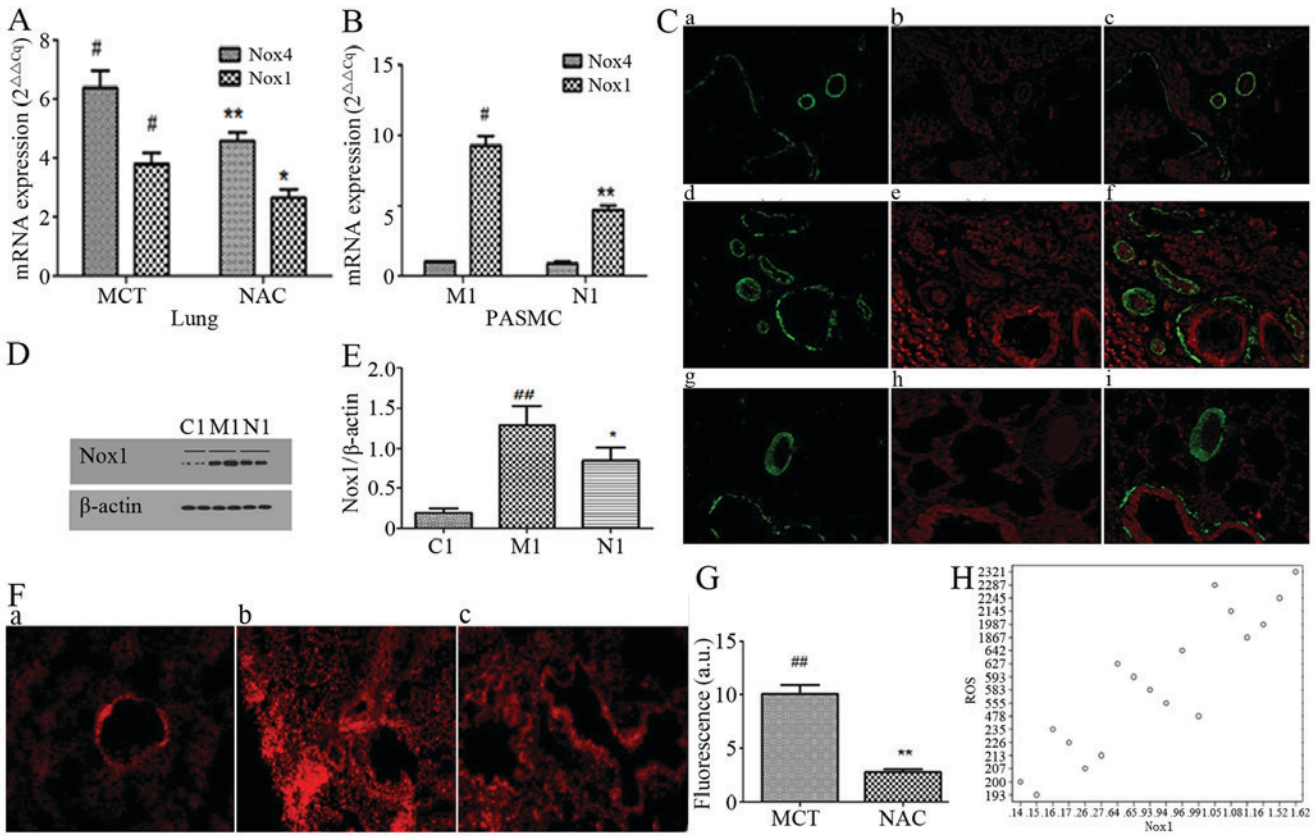

Figure 2. Expression of Nox 1 and Nox4. (A) The mRNA level of Nox1 and Nox4 in lung tissue. The standardization of group Cont was 1. #P<0.05 vs. Cont; *P<0.05 vs. MCT; **P<0.001 vs. MCT. (B) The mRNA level of Nox1 and Nox4 in PASMCs. The standardization of group Cont was 1. $P<0.05 vs. C1; +P<0.001 vs. M1. (C) Double immunofluorescence staining of Nox1 and α-SMA in lung tissue. Green, α-SMA; red, Nox1. (D) Western blotting and (E) densitometric analysis of the expression of Nox1 protein in PASMCs (n=6). β-actin was used as the internal control. $$P<0.001 vs. C1; ++P=0.011 vs. M1. (F) DHE fluorescence intensity of the lung tissue. (G) The standardization of group Cont was 1. The data demonstrate the fold change of group MCT and group NAC relative to group Cont. ##P<0.001 vs. Cont; **P<0.001 vs. MCT. (H) Correlation analysis of Nox1 and DHE fluorescence intensity. r=0.850; P<0.001. PASMC, pulmonary artery smooth muscle cell; Nox, NADPH oxidase; Cont, control; α-SMA, smooth muscle actin; MCT, monocrotaline; NAC, N-acetylcysteine; M, MCT-treated; N, NAC-treated group; C, control subgroup; DHE, dihydroethidium.

the process of PVR, and whether the effects are beneficial or harmful, in addition to the specific source, remains to be elucidated (13). In addition to hypoxia-induced PH, the same questions in non-hypoxia-induced PH remain unresolved.

Experiments prior to the present study, and the study by Ahmad *et al* (14) demonstrated that an increase in Nox4-derived ROS may lead to PVR in hypoxia-induced PAH. Seta *et al* (15) reported that Nox4 was increased in MCT-PH rats. An additional study demonstrated that the excessive proliferation and migration of PASMCs in MCT-PH was caused by the Nox1-derived oxidation imbalance (4). In the present study, the mRNA and corresponding protein expression of Nox1 and Nox4 in the lung tissues of the MCT-treated group were increased compared with the control group, and NAC was able to downregulate the expression of Nox1 and Nox4. However, the mRNA samples extracted from PASMCs exhibited increased expression of Nox1 only, and the α-SMA fluorescence intensity used to measure the extent of vascular muscularization was significantly positively correlated with the expression level of Nox1, consistent with Veit *et al* (5). These observations may be associated with the fact that experiments performed prior to the present study used the hypoxia-induced PH model, and the samples in the study by Seta *et al* (15) originated from lung tissue homogenates, indicating that different modeling methods and different tissues may exhibit have different Nox isoforms. In PASMCs, Nox4 and Nox1 were dominant, and the endothelial cells appeared to be the primary location for the functioning of Nox4; however, the expression of Nox1 appeared to be limited in PASMCs and maintained at low concentrations in other vascular cells (16,17), and this was the reason why Nox1 was less well-studied in cardiovascular research compared with Nox4 (18,19).

In hypoxic PASMCs isolated from chronically hypoxic mice, the expression of Nox4 was demonstrated to be increased (20,21). Following treatment with MCT, the expression level of Nox1 mRNA was significantly increased in PASMCs, although the expression of Nox4 did not change, which was associated with the different activation methods and distributions of Nox1 and Nox4 in addition to different pathogeneses of PH. In contrast to hypoxia-induced PH, the injection of MCT largely caused the secretion of inflammatory factors, including platelet-derived growth factors, thereby leading to strong inflammatory responses. These inflammatory cytokines were able to stimulate an increased in the expression and activity of Nox1 (22). NAC produces its MCT-PH protective effects through anti-inflammatory and immunomodulatory mechanisms (9-11). The present study compared pulmonary arterial pressure and PVR in the MCT

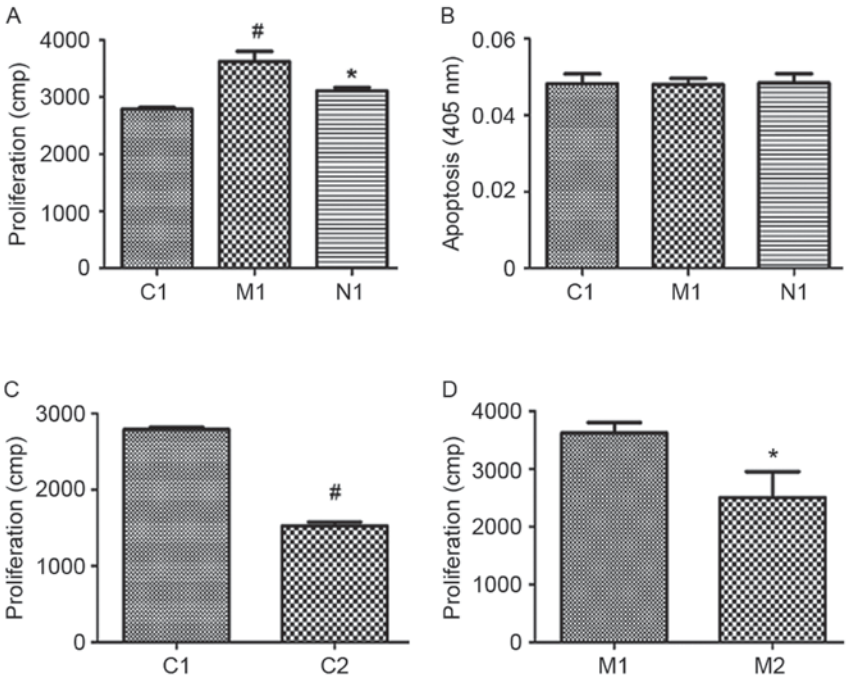

Figure 3. Proliferation and apoptosis assays in PASMCs. (A) The proliferation of PASMCs from groups C, M and N. #P<0.001 vs. C1; *P<0.001 vs. M1. (B) The apoptosis of PASMCs from groups C, M and N. (C) The proliferation of group C prior to and following treatment with ML171. #P<0.001 vs. C1. (D) The proliferation of group M prior to and following treatment with ML171. *P<0.001 vs. M1. PASMC, pulmonary artery smooth muscle cell. C, control; M, monocrotaline-treated; N, N-acetylcysteine-treated.

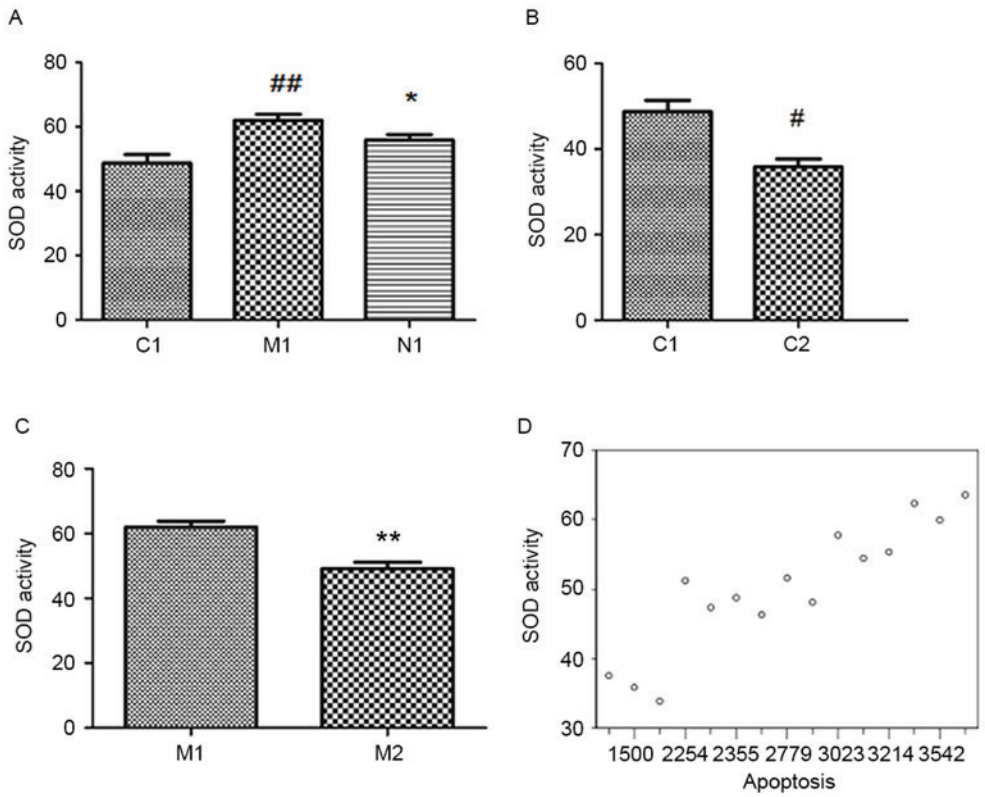

Figure 4. Analysis of SOD activity. (A) The total activity of SOD in PASMCs. ##P<0.001 vs. C1; *P=0.012 vs. M1. (B) The total SOD activity in group C prior to and following treatment with ML171. #P=0.002 vs. C1. (C) The total SOD activity in group M prior to and following treatment with ML171. **P=0.001 vs. M1. (D) Correlation analysis of the total SOD activity and the proliferation of PASMCs. r=0.949; P<0.001. SOD, superoxide dismutase; PASMC, pulmonary artery smooth muscle cell; C, control; M, monocrotaline-treated; N, N-acetylcysteine-treated.

and NAC groups, and further validated the conclusion that NAC acts via anti-inflammatory and immunomodulatory mechanisms; in addition, it was demonstrated from one lateral side that, different from hypoxia-induced PH,

MCT-PASMCs exhibited Nox1-mediated regulation of cell proliferation rather than Nox4, and this was caused by different upstream stimulatory factors mediating different signaling pathways. Nox4 appeared to be primarily associated with hypoxia-induced PH, and Nox1 with inflammation and immune stimulation-induced PH.

It has been hypothesized that oxidative stress induces inflammation, and that the inhibition of ROS enzymes (such as Nox) and SOD may effectively decrease *in vivo* and *in vitro* inflammation (23,24). It has been suggested that inflammation may induce oxidative stress and that Nox complexes serve key roles in this process (25). Therefore, the association between Nox and inflammation-induced oxidative stress may be defined as a vicious cycle, leading to vascular disease. In MCT-PH, in addition to the increase in ROS-represented oxidative levels, the antioxidant capacity may additionally be increased. In the present study, it was specifically demonstrated that, compared with group C1, the SOD activity in the PASMCs of group M1 was significantly increased; following treatment with the Nox1 inhibitor ML171, the generation of SOD returned to normal levels, and the proliferation of MCT-PASMCs was significantly decreased. The correlation analysis demonstrated that these two factors were strongly correlated, indicating that SOD served important roles via the Nox1-SOD signaling pathway.

Analysis of the correlation between Nox1 and DHE demonstrated that when the Nox1-derived O_2^- was increased, the SOD activity was additionally increased; it was therefore hypothesized that the downstream signaling molecule of this process was H_2O_2. Analysis of the correlation between SOD activity and the proliferation of smooth muscle cells, in addition to the alterations in SOD activity, led to the hypothesis that the Nox-derived O_2^- may produce more H_2O_2 following dismutation by SOD, and that the latter served roles as an intra- and extracellular messenger (26). H_2O_2 could react with cysteine in a reversible manner. H_2O_2 may lead to the decreased production of NO, and may additionally release intracellular Ca^{2+} and contract pulmonary vessels (16). The results of the present study, demonstrating that the total SOD activity in group N1 was significantly decreased compared with group M1, additionally demonstrated that NAC may exert functions on MCT-PASMCs by affecting the Nox1-SOD signaling pathway, rather than by increasing the antioxidant capacities so as to decrease ROS formation. Nox1 exhibited different intervention targets in MCT-PH models, and in other animal and human PH models, and this requires further study.

In conclusion, in lung tissues, Nox1 and Nox4 were associated with the formation of PAH, and NAC was able to serve therapeutic roles by decreasing the expression of Nox1 and Nox4. In PASMCs, NAC was able to improve PVR by reducing Nox1-, rather than Nox4-, derived ROS to reduce the proliferation of smooth muscle cells, thereby reducing pulmonary arterial pressure and RVH. The promotive roles of Nox1-derived ROS on the proliferation of smooth muscle cells may be achieved by increasing SOD and the downstream signaling molecule H_2O_2. The generation site, type and downstream-involved oxidation and antioxidation imbalances of Nox have not been demonstrated to be consistent in different studies; thus, further studies are required in order to elucidate the accurate mechanisms. In the present study, ML171 was less of a focus; therefore, the results of the present study require verification by gene knockout or inhibition studies prior to this research being translated into clinical practice.

References

1. Galiè N, Humbert M, Vachiery JL, Gibbs S, Lang I, Torbicki A, Simonneau G, Peacock A, Vonk Noordegraaf A, Beghetti M, *et al*: 2015 ESC/ERS Guidelines for the diagnosis and treatment of pulmonary hypertension: The Joint Task Force for the Diagnosis and Treatment of Pulmonary Hypertension of the European Society of Cardiology (ESC) and the European Respiratory Society (ERS): Endorsed by: Association for European Paediatric and Congenital Cardiology (AEPC), International Society for Heart and Lung Transplantation (ISHLT). Eur Heart J 37: 67-119, 2016.
2. Qiao S, Fan K, Iwashita T, Ichihara M, Yoshino M and Takahashi M: The involvement of reactive oxygen species derived from NADPH oxidase-1 activation on the constitutive tyrosine auto-phosphorylation of RET proteins. Free Radic Res 48: 427-434, 2014.
3. Schermuly RT, Ghofrani HA, Wilkins MR and Grimminger F: Mechanisms of disease: Pulmonary arterial hypertension. Nat Rev Cardiol 8: 443-455, 2011.
4. Freund-Michel V, Guibert C, Dubois M, Courtois A, Marthan R, Savineau JP and Muller B: Reactive oxygen species as therapeutic targets in pulmonary hypertension. Ther Adv Respir Dis 7: 175-200, 2013.
5. Veit F, Pak O, Egemnazarov B, Roth M, Kosanovic D, Seimetz M, Sommer N, Ghofrani HA, Seeger W, Grimminger F, *et al*: Function of NADPH oxidase 1 in pulmonary arterial smooth muscle cells after monocrotaline-induced pulmonary vascular remodeling. Antioxid Redox Signal 19: 2213-2231, 2013.
6. Ismail S, Sturrock A, Wu P, Cahill B, Norman K, Huecksteadt T, Sanders K, Kennedy T and Hoidal J: NOX4 mediates hypoxia-induced proliferation of human pulmonary artery smooth muscle cells: The role of autocrine production of transforming growth factor-{beta}1 and insulin-like growth factor binding protein-3. Am J Physiol Lung Cell Mol Physiol 296: L489-L499, 2009.
7. Wassmann S, Wassmann K and Nickenig G: Modulation of oxidant and antioxidant enzyme expression and function in vascular cells. Hypertension 44: 381-386, 2004.
8. Millea PJ: N-acetylcysteine: Multiple clinical applications. Am Fam Physician 80: 265-269, 2009.
9. Kelly GS: Clinical applications of N-acetylcysteine. Altern Med Rev 3: 114-127, 1998.
10. Santus P, Corsico A, Solidoro P, Braido F, Di Marco F and Scichilone N: Oxidative stress and respiratory system: Pharmacological and clinical reappraisal of N-acetylcysteine. COPD 11: 705-717, 2014.
11. Chaumais MC, Ranchoux B, Montani D, Dorfmüller P, Tu L, Lecerf F, Raymond N, Guignabert C, Price L, Simonneau G, *et al*: N-acetylcysteine improves established monocrotaline-induced pulmonary hypertension in rats. Respir Res 15: 65, 2014.
12. Livak KJ and Schmittgen TD: Analysis of relative gene expression data using real-time quantitative PCR and the 2(-Delta Delta C(T)) method. Methods 25: 402-408, 2001.
13. Veit F, Pak O, Brandes RP and Weissmann N: Hypoxia-dependent reactive oxygen species signaling in the pulmonary circulation: Focus on ion channels. Antioxid Redox Signal 22: 537-552, 2015.
14. Ahmad M, Kelly MR, Zhao X, Kandhi S and Wolin MS: Roles for Nox4 in the contractile response of bovine pulmonary arteries to hypoxia. Am J Physiol Heart Circ Physiol 298: H1879-H1888, 2010.
15. Seta F, Rahmani M, Turner PV and Funk CD: Pulmonary oxidative stress is increased in cyclooxygenase-2 knockdown mice with mild pulmonary hypertension induced by monocrotaline. PLoS One 6: e23439, 2011.
16. Briones AM and Touyz RM: Oxidative stress and hypertension: Current concepts. Curr Hypertens Rep 12: 135-142, 2010.
17. Guzik TJ, Sadowski J, Guzik B, Jopek A, Kapelak B, Przybylowski P, Wierzbicki K, Korbut R, Harrison DG and Channon KM: Coronary artery superoxide production and nox isoform expression in human coronary artery disease. Arterioscler Thromb Vasc Biol 26: 333-339, 2006.
18. Cheng G and Lambeth JD: NOXO1, regulation of lipid binding, localization, and activation of Nox1 by the Phox homology (PX) domain. J Biol Chem 279: 4737-4742, 2004.

19. Helmcke I, Heumüller S, Tikkanen R, Schröder K and Brandes RP: Identification of structural elements in Nox1 and Nox4 controlling localization and activity. Antioxid Redox Signal 11: 1279-1287, 2009.
20. Diebold I, Petry A, Hess J and Görlach A: The NADPH oxidase subunit NOX4 is a new target gene of the hypoxia-inducible factor-1. Mol Biol Cell 21: 2087-2096, 2010.
21. Judkins CP, Diep H, Broughton BR, Mast AE, Hooker EU, Miller AA, Selemidis S, Dusting GJ, Sobey CG and Drummond GR: Direct evidence of a role for Nox2 in superoxide production, reduced nitric oxide bioavailability, and early atherosclerotic plaque formation in ApoE-/- mice. Am J Physiol Heart Circ Physiol 298: H24-H32, 2010.
22. Yin W and Voit EO: Function and design of the Nox1 system in vascular smooth muscle cells. BMC Syst Biol 7: 20, 2013.
23. Valdivia A, Pérez-Alvarez S, Aroca-Aguilar JD, Ikuta I and Jordán J: Superoxide dismutases: A physiopharmacological update. J Physiol Biochem 65: 195-208, 2009.
24. Jaulmes A, Sansilvestri-Morel P, Rolland-Valognes G, Bernhardt F, Gaertner R, Lockhart BP, Cordi A, Wierzbicki M, Rupin A and Verbeuren TJ: Nox4 mediates the expression of plasminogen activator inhibitor-1 via p38 MAPK pathway in cultured human endothelial cells. Thromb Res 124: 439-446, 2009.
25. Anrather J, Racchumi G and Iadecola C: NF-kappaB regulates phagocytic NADPH oxidase by inducing the expression of gp91phox. J Biol Chem 281: 5657-5667, 2006.
26. Schröder E and Eaton P: Hydrogen peroxide as an endogenous mediator and exogenous tool in cardiovascular research: Issues and considerations. Curr Opin Pharmacol 8: 153-159, 2008.